Optical Imaging of Bacterial Infection in Living Mice Using a Fluorescent Near-Infrared Molecular Probe

W. Matthew Leevy,[†,‡] Seth T. Gammon,[§] Hua Jiang,[†,||] James R. Johnson,[†] Dustin J. Maxwell,[§] Erin N. Jackson,[§] Manuel Marquez,[⊥,#,▽] David Piwnica-Worms,[§] and Bradley D. Smith*[,†]

Department of Chemistry and Biochemistry, 251 Nieuwland Science Hall, University of Notre Dame, Notre Dame, Indiana 46556, Interdisciplinary Network of Emerging Science and Technologies (NEST) Group Postgraduate Program and Research Center, Philip Morris USA, 4201 Commerce Road, Richmond, Virginia 23234, Molecular Imaging Center, Mallinckrodt Institute of Radiology, Washington University School of Medicine, 510 South Kingshighway Boulevard, Campus Box 8225, St. Louis, Missouri 63110, Key Laboratory of Photochemistry, Institute of Chemistry, Chinese Academy of Sciences, Beijing 100080, China, NIST Center for Theoretical and Computational Nanosciences, Gaithersburg, Maryland 20899, and Harrington Department of Bioengineering, Arizona State University, Tempe, Arizona 85287

Received September 14, 2006; E-mail: smith.115@nd.edu

Bacterial imaging is an emerging technology that has many health and environmental applications.[1] For example, there is an obvious need to develop highly sensitive assays that can detect very small numbers of pathogenic bacterial cells in food, drinking water, or biomedical samples. In other situations, the goal is to study in vivo the temporal and spatial distribution of bacteria in live animals.

Optical imaging of bacteria in vivo is much less developed than methods such as radioimaging and MRI. One approach is to use bacteria that are genetically encoded to produce luciferase or green fluorescent protein.[2] A second strategy, which is the focus of this study, employs a molecular probe with a fluorescent reporter group. An obvious limitation with a live animal is restricted tissue penetration of the light. However, near-infrared (NIR) dyes with emission wavelengths in the region of 650−900 nm can propagate through two or more centimeters of tissue and may enable deeper tissue imaging if sensitive detection techniques are employed.[3] Compared to MRI and radioimaging, optical imaging provides a convenient method to monitor multiple biological processes simultaneously and in real time.[4] Furthermore, the technology is operationally simple, amenable to miniaturization, and potentially mobile.

Molecular imaging probes can often be deconstructed into two structural components, an affinity ligand and a reporter group. In the case of bacterial targeting, previously reported affinity ligands include antibodies,[5] sugars,[6] bacteria binding peptides,[7] antimicrobial peptides,[8] enzyme substrates,[9] and antibiotic drugs.[10] Recently, we discovered that fluorescent molecular probes containing synthetic zinc(II) dipicolylamine (Zn-DPA) coordination complexes as affinity groups are able to selectively stain the surfaces of bacterial cells[11] and apoptotic animal cells.[12] Zn-DPA affinity ligands bind strongly to the anionic surfaces that are a common characteristic of these two cell types, whereas affinity for the zwitterionic surfaces of healthy animal cells is weak. These in vitro results have motivated us to pursue in vivo studies, and we report that molecular probe **1**, which has a NIR fluorophore attached to an affinity group with two Zn-DPA units, can be used for targeted, fluorescence imaging of bacterial infection in a living whole animal.

The bacterial imaging probe **1** (λ_{max} abs: 794 nm, em: 810 nm)

was prepared in straightforward fashion using a carbocyanine dye as the NIR fluorophore.[13] Researchers have incorporated this fluorophore into probes for other optical imaging applications.[14] In vitro fluorescence microscopy studies proved that probe **1** can effectively stain the periphery of bacterial cells (Figure 1). In contrast, the cells are not stained when treated under identical conditions with control fluorophore **2**, confirming that the Zn-DPA affinity group is required for bacteria cell targeting.
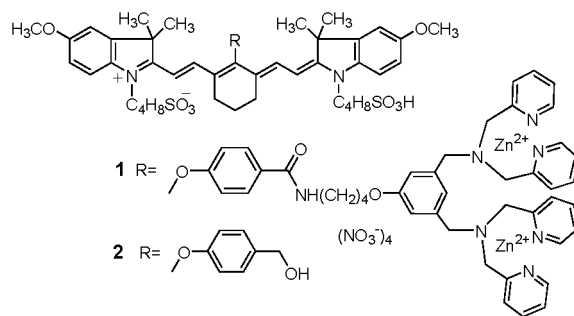
With these results in hand, we progressed to in vivo imaging of nude mice that were infected with injections of Gram-positive *Staphylococcus aureus* NRS11. Imaging was achieved by placing an anesthetized mouse inside a Kodak 4000MM imaging station configured for epi-illumination. The entire animal was irradiated with filtered light of wavelength 720 ± 35 nm and an image of emission intensity at 790 ± 35 nm was collected by a CCD camera during a 60 s acquisition period.[15] First, we examined a series of mice with thigh muscle injections of bacteria that were preincubated with NIR probe **1** or control fluorophore **2**. As shown in Figure 1, the fluorescence from the bacteria treated with **1** can easily penetrate through the skin and muscle tissue of the living animal. Fluorescence was not detected at the site that was injected with cells that were preincubated with **2**.[16]

Next, we conducted in vivo targeting experiments, where the bacteria were injected into the mouse thigh, and fluorescent probe was introduced into the bloodstream. The images in Figure 2 show the change in fluorescence intensity emanating from one mouse, out of a cohort of four, with a *S. aureus* NRS11 infection (∼5 × 10^{7} colony forming units in 50 μL Luria Bertani (LB) broth) in the left rear thigh. The opposite side of the mouse was injected with only the LB vehicle as a negative control. The infections were allowed to incubate for 6 h, followed by introduction of probe **1** (75 μL of 1 mM aqueous stock solution) into the blood stream via

† University of Notre Dame.
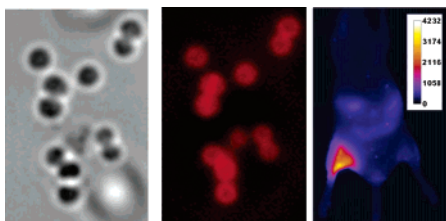‡ INEST Group Postgraduate Program, Philip Morris.
§ Washington University School of Medicine.
|| Chinese Academy of Sciences.
⊥ NIST Center for Theoretical and Computational Nanosciences.
Arizona State University.
▽ Research Center, Philip Morris.

Figure 1. (Left) Phase contrast image of *S. aureus* cells treated with probe **1** (10 *μ*M) and viewed at 1500×. (Middle) Fluoresence image of the same cells acquired with a Cy7 filter set. (Right) Fluorescence image of a live mouse after thigh muscle injections of *S. aureus* cells that were preincubated for 5 min with 10 *μ*M of either **1** or **2** (left and right leg, respectively). Scale represents relative fluorescence intensity in arbitrary units.
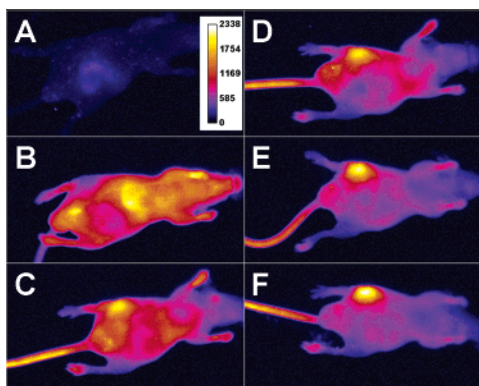
Figure 2. Optical images of a mouse with a *S. aureus* infection in the left rear thigh muscle. Images were acquired before (A), and immediately following (B), intravenous injection of probe **1** and at 6 h (C), 12 h (D), 18 h (E), and 21 h (F). Scale represents the same relative fluorescence intensity for all six images in arbitrary units.

a tail vein injection. Panels A and B show the mouse immediately before and following injection of **1**. The fluorescent probe clears slowly from the blood stream, except for significant accumulation at the site of bacterial infection. The maximum signal contrast is reached after about 18 h (panels E and F). With this cohort of four mice, the in vivo fluorescence intensity from the infected muscle after 21 h was 3.7 ± 0.6 times higher than the contralateral control muscle.[17] Similar imaging results were obtained with mice that were infected with *Escherichia coli* (see Supporting Information). As expected, control studies using mice injected with the fluorophore **2** failed to show localized emission from the site of bacterial infection (data not shown). These bacteria targeting experiments have been repeated successfully on several separate occasions using different cohorts of nude mice, independent batches of the probe **1**, and different workers performing the infection and imaging procedures. A residual fluorescence signal from the tail of the mouse is often observed, since it is the point of injection of **1**. Another notable observation is the mice (infected or uninfected) appear to easily tolerate the presence of probe **1** over the 21 h time-course of these experiments, as judged by their continued grooming and nesting activities.

These in vivo imaging results are in accord with our previous in vitro observations that appropriately designed Zn-DPA coordination complexes have a strong and selective affinity for anionic bacterial cells over healthy animal cells.[11] It is also possible that probe **1** is targeting the adjacent apoptotic/necrotic tissue that is produced by the bacteria's virulent action.[18] Ongoing histology experiments will address this question.

In summary, the NIR fluorescent probe **1** selectively accumulates at bacterial infection sites in the thigh muscles of nude mice. Future studies will determine if it is possible to image more medically relevant infection sites that are within the tissue penetration limit

for NIR light (e.g., skin, throat, urinary tract, etc). Another goal is to conjugate affinity groups containing Zn-DPA units to other types of imaging reporter groups or therapeutic agents and produce a range of useful probes for various in vivo imaging and pharmaceutical applications.

Supporting Information Available: Synthetic and experimental details. This material is available free of charge via the Internet at http://pubs.acs.org.

References

(1) Bleeker-Rovers, C. P.; Boerman, O. C.; Rennen, H. J. J.; Corstens, F. H. M.; Oyen, W. J. G. *Curr. Pharm. Des.* **2004**, *10*, 2935−2950.

(2) (a) Sato, A.; Klaunberg, A.; Tolwani, R. *Comp. Med.* **2004**, *54*, 631−634. (b) Doyle, T. C.; Burns, S. M.; Contag, C. H. *Cell. Microbiol.* **2004**, *6*, 303−317.

(3) (a) Licha, K. *Top. Curr. Chem.* **2002**, *222*, 1−29. (b) Achilefu, S. *Technol. Cancer Res. Treat.* **2004**, *3*, 393−409. (c) Sevick-Muraca, E. M.; Houston, J. P.; Gurfinkel, M. *Curr. Opin. Chem. Biol.* **2002**, *6*, 642−650.

(4) Gross, S.; Piwnica-Worms, D. *Cancer Cell* **2005**, *7*, 5−15.

(5) Zhao, X.; Hilliard, L. R.; Mechery, S. J.; Wang, Y.; Bagwe, R. P.; Jin, S.; Tan, W. *Proc. Nat. Acad. Sci. U.S.A.* **2004**, *101*, 15027−15032.

(6) Qu, L. W.; Luo, P. G.; Taylor, S.; Lin, Y.; Huang, W. J.; Anyadike, N.; Tzeng, T. R. J.; Stutzenberger, F.; Latour, R. A.; Sun, Y. P. *J. Nanosci. Nanotechnol.* **2005**, *5*, 319−322.

(7) Dhayal, B.; Henne, W. A.; Doorneweerd, D. D.; Reifenberger, R. G.; Low, P. S. *J. Am. Chem. Soc.* **2006**, *128*, 3716−3721.

(8) Lupetti, A. L.; Wellng, M. M.; Pauwels, E. K. J.; Nibbering, P. H. *Lancet* **2003**, *3*, 223−229.

(9) Bettegowda, C.; Foss, C. A.; Cheong, I.; Wang, Y.; Diaz, L.; Agrawal, N.; Fox, J.; Dick, J.; Dang, L. H.; Zhou, S.; Kinzler, K. W.; Vogelstein, B.; Pomper, M. G. *Proc. Natl. Acad. Sci. U.S.A.* **2005**, *102*, 1145−1150.

(10) Britton, K. E.; Wareham, D. W.; Das, S. S.; Solanki, K. K.; Amaral, H.; Bhatnagar, A.; Katamihardja, A. H. S.; Malamitsi, J.; Moustafa, H. M.; Soroa, V. E.; Sundram, F. X.; Padhy, A. K. *J. Clin. Path.* **2002**, *55*, 817−823.

(11) Leevy, W. M.; Johnson, J. R.; Lakshmi, C.; Morris, J.; Marquez, M.; Smith, B. D. *Chem. Commun.* **2006**, 1595−1597.

(12) Hanshaw, R. G.; Lakshmi, C.; Lambert, T. N.; Johnson, J. R.; Smith, B. D. *ChemBioChem* **2005**, *12*, 2214−2220.

(13) Narayanan, N.; Patonay, G. *J. Org. Chem.* **1995**, *60*, 2391−95.

(14) (a) Zaheer, A.; Wheat, T. E.; Frangioni, J. V. *Mol. Imaging* **2002**, *1*, 354−364 and references therein. (b) Zhang, Z.; Achilefu, S. *Org. Lett.* **2004**, *6*, 2067−2070.

(15) The in vivo imaging data reported in this paper was acquired with the Cy7 filter set recommended by the manufacturer. Efforts to optimize the filter set for probe **1** are ongoing.

(16) In vitro measurements of minimum inhibitory concentration (MIC) showed no inhibition of *S. aureus* growth by probe **1** or fluorophore **2** at the maximum tested concentrations of 100 and 400 *μ*M, respectively. Furthermore, fluorescence microscopy of *S. aureus* cells grown to confluence in the presence of probe **1** showed no time-dependent change in probe staining intensity or staining location (bacterial cell periphery).

(17) The uncertainty is the standard error of the mean from region of interest analysis of the infected and uninfected thigh. At 21 h, each mouse was sacrificed and dissected to confirm selective accumulation in the infected thigh muscle. The complete tissue distribution profile is provided in the supporting information.

(18) The Zn-DPA affinity group has a strong affinity for anionic membrane surfaces that are rich in amphiphilic phosphates (see, O Neil, E. J.; Smith, B. D. *Coord. Chem. Rev.* **2006**, *250*, 3068-3080). On average, the surfaces of healthy animal cells are zwitterionic, whereas, the surfaces of apoptotic animal cells are anionic because of the translocation of phosphatidylserine from the inner to the outer leaflet of the cell-plasma membrane. The four most likely anionic targets in the bacterial cell wall are lipid A, the phosphorylated membrane anchor component of lipopolysaccharide that resides in the outer monolayer of the outer membrane of Gram-negative bacteria; lipoteichoic acid, an amphiphilic glycerophosphate polymer that extends from the surface of Gram-positive bacteria; and two anionic phospholipids, phosphatidylglycerol and cardiolipin which constitute a large fraction of the total pool of membrane phospholipids. A related question is whether the Zn^{2+} cations in probe **1** exchange with other transition metal cations that are physiologically present and available. This is a difficult question to address unambiguously, but it is known that *E. coli* are enriched in several transition metals including Zn, Fe, Cu, and Mn, although they are primarily sequestered in binding sites of various affinities. Finney, L. A.; O Halloran, T. V. *Science* **2003**, *300*, 931-936.

JA0665592